Article

DNA Hybridization-Induced Reorientation of Liquid Crystal Anchoring at the Nematic Liquid Crystal/Aqueous Interface

Andrew D. Price, and Daniel K. Schwartz

J. Am. Chem. Soc., **2008**, 130 (26), 8188-8194 • DOI: 10.1021/ja0774055 • Publication Date (Web): 04 June 2008

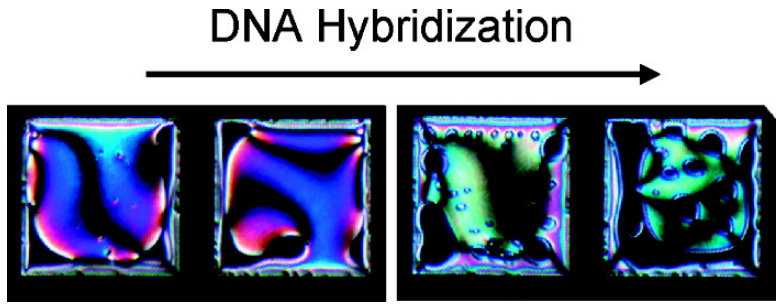

J|A|C|S
ARTICLES

Published on Web 06/04/2008

DNA Hybridization-Induced Reorientation of Liquid Crystal Anchoring at the Nematic Liquid Crystal/Aqueous Interface

Andrew D. Price and Daniel K. Schwartz*

University of Colorado, Department of Chemical and Biological Engineering, Boulder, Colorado 80309-0424

Received September 25, 2007; Revised Manuscript Received April 14, 2008; E-mail: daniel.schwartz@colorado.edu

Abstract: Interactions between DNA and an adsorbed cationic surfactant at the nematic liquid crystal (LC)/aqueous interface were investigated using polarized and fluorescence microscopy. The adsorption of octadecyltrimethylammonium bromide (OTAB) surfactant to the LC/aqueous interface resulted in homeotropic (untilted) LC alignment. Subsequent adsorption of single-stranded DNA (ssDNA) to the surfactant-laden interface modified the interfacial structure, resulting in a reorientation of the LC from homeotropic alignment to an intermediate tilt angle. Exposure of the ssDNA/OTAB interfacial complex to its ssDNA complement induced a second change in the interfacial structure characterized by the nucleation, growth, and coalescence of lateral regions that induced homeotropic LC alignment. Fluorescence microscopy showed explicitly that the complement was colocalized in the same regions as the homeotropic domains. Exposure to noncomplementary ssDNA caused no such response, suggesting that the homeotropic regions were due to DNA hybridization. This hybridization occurred in the vicinity of the interface despite the fact that the conditions in bulk solution were such that hybridization did not occur (high stringency), suggesting that the presence of the cationic surfactant neutralized electrostatic repulsion and allowed for hydrogen bonding between DNA complements. This system has potential for label-less and portable DNA detection. Indeed, LC response to ssDNA target was detected with a lower limit of ~50 fmol of complement and was sufficiently selective to differentiate a one-base-pair mismatch in a 16-mer target.

Introduction

Thermotropic liquid crystals (LCs) have demonstrated utility in the transduction of molecular events at an interface into macroscopic responses visible with the naked eye.[1–8] The orientation of LC molecules is extraordinarily sensitive to physical and chemical properties of a bounding interface, and the long-range order inherent in LC phases serves to amplify surface-induced ordering for macroscopic distances. These properties, combined with the optical anisotropy of LC molecules, make them well-suited for the direct transduction and amplification of the binding of an analyte to a target at an interface into an optical output.[5,8,9] Unlike most current methods for the detection of biological analytes, which generally require laboratory-based analytical detectors and labeled species such as fluorophores or radioactive isotopes,[10] LC-based detection may be carried out in ambient light without the need for electrical power or molecular labels. This makes LC-based detection particularly useful for detection assays performed away from central laboratory locations including point-of-care, home-based, and field-based assays.

The principles of LC-based detection rely on optical, anchoring, and elastic properties arising from molecular anisotropies and the unique liquid-crystalline phase of the LC material.[11] The molecular anisotropy of a liquid crystalline sample creates a difference in the refractive indices of light parallel and perpendicular to the bulk molecular orientation, i.e., the LC director.[12] This difference, known as birefringence, creates a discernible optical signal that is lost when the director orients parallel to the direction of light propagation. Molecular-scale interactions between an LC and a neighboring interface result in a preferred anchoring angle relative to the surface normal.[13] Information about the interface, in the form of surface anchoring, is transmitted as far as 100 μm into the bulk[8] as a result of the elastic nature of the LC director field.

(1) Brake, J. M.; Abbott, N. L. *Langmuir* **2007**, *23*, 8497–8507.
(2) Park, J.-S.; Teren, S.; Tepp, W. H.; Beebe, D. J.; Johnson, E. A.; Abbott, N. L. *Chem. Mater.* **2006**, *18*, 6147–6151.
(3) Clare, B. H.; Abbott, N. L. *Langmuir* **2005**, *21*, 6451–6461.
(4) Kim, H.-R.; Kim, J.-H.; Kim, T.-S.; Oh, S.-W.; Choi, E.-Y. *Appl. Phys. Lett.* **2005**, *87*, 143901.
(5) Brake, J. M.; Daschner, M. K.; Luk, Y.-Y.; Abbott, N. L. *Science* **2003**, *302*, 2094–2097.
(6) Luk, Y.-Y.; Tingey, M. L.; Hall, D. J.; Israel, B. A.; Murphy, C. J.; Bertics, P. J.; Abbott, N. L. *Langmuir* **2003**, *19*, 1671–1680.
(7) Kim, S.-R.; Abbott, N. L. *Langmuir* **2002**, *18*, 5269–5276.
(8) Gupta, V. K.; Skaife, J. J.; Dubrovsky, T. B.; Abbott, N. L. *Science* **1998**, *279*, 2077–2080.
(9) Hoogboom, J.; Clerx, J.; Otten, M. B. J.; Rowan, A. E.; Rasing, T.; Nolte, M. *Chem. Commun.* **2003**, *2856*, 2857.
(10) Blum, L. J.; Coulet, P. R. *Biosensor Principles and Applications*; Marcel Dekker: New York, 1991.
(11) de Gennes, P. J.; Prost, J. *The Physics of Liquid Crystals*, 2nd ed.; Oxford University Press: New York, 1995.
(12) Dunmur, D.; Fukuda, A.; Luckhurst, G. R. *Physical Properties of Liquid Crystals: Nematics*; INSPEC, Institution of Electrical Engineers: London, 2001.
(13) Rasing, T.; Musevic, I. *Surfaces and Interfaces of Liquid Crystals*; Springer: Berlin, 2004.

10.1021/ja0774055 CCC: $40.75

Coupling the structure of the interface to a bioreaction, such as molecular recognition, may cause a bulk reorientation of the LCs as the reaction proceeds, generating an optical signal.[1,5] The aqueous/LC interface is particularly interesting in this regard, because the aqueous phase permits convenient molecular transport to the interface and the fluidity of the interface allows for rapid, large-scale lateral molecular rearrangements. Furthermore, the chemical properties of the interface can be modified in a controlled way by adsorption of a surfactant.[14,15] In the absence of surfactant, a highly tilted (nearly planar) LC orientation is observed. At sufficient surfactant coverage, the tilted anchoring at the interface reorients to a homeotropic alignment.[14,16] We have previously shown that long-chain *n*-alkanoic acids adsorbed at the aqueous/LC interface possess distinct 2D phases dependent on the surfactant chemical potential and the temperature of the interface[14] that are reminiscent of fatty acid monolayer phases at the air/water interface.[17] LC anchoring is sensitive to the subtle structural differences between these phases. Previous work suggested that while LC interactions with surfactant tails are responsible for anchoring, electrostatic interactions of the surfactant headgroups affect the interfacial density of the surfactant monolayer,[18] thereby controlling the LC anchoring indirectly. The premise of the work presented in this manuscript is that changing the nature of the headgroups through noncovalent interactions with biomolecules can drive structural transitions via supramolecular chemistry.

Deoxyribonucleic acid (DNA) has long been known to form insoluble complexes with cationic surfactants in aqueous environments.[19] In some cases, the complexes form highly ordered lamellar structures, with DNA intercalated between surfactant bilayers.[20] Research into DNA−lipid complexes has been predominantly driven by expectations of their use as nonviral gene carriers in transfection applications[20–22] and in molecular diagnostics.[23] Despite the promise of DNA/lipid complexes, DNA interactions with charged surfaces remain poorly understood.[24] The use of Langmuir monolayers of cationic lipids has provided one method for probing DNA at such surfaces.[23–30] Möhwald et al. have shown that DNA binding to a cationic phospholipid monolayer condenses the membrane surface.[28] Furthermore, Sastry et al. measured molecular area changes upon hybridization of an oligomer target to membrane-bound DNA probes at the air/water interface,[23,27] and Sukhorukov et al. showed that double-stranded DNA (dsDNA) does not denature upon adsorbing to a cationic surfactant monolayer at a similar interface.[25]

In this study we investigate DNA interactions with a cationic surfactant adsorbed at an LC/aqueous interface. This experimental geometry, which builds upon a setup first demonstrated by Abbott and co-workers,[31] provides a way to probe interactions between DNA and cationic surfaces due to the sensitivity of LC anchoring to the structure of the interface. We find that DNA hybridization occurs at this interface even under solution conditions of high stringency, where hybridization in bulk solution is frustrated by electrostatic repulsion. This interfacial hybridization is highly selective and results in changes to the interfacial structure that induces LC molecular reorientation. This has potential as a sensitive and specific label-less DNA detection platform.

Experimental Details

LC Film Preparation. Borosilicate glass slides were cleaned with a fresh piranha solution composed of 30% aqueous H_2O_2 and concentrated H_2SO_4 (1:3 v/v) for 1 h at 70 °C. (**Warning: piranha solution reacts strongly with organic compounds and should be handled with extreme caution; do not store solution in closed containers**.) An octadecyltriethoxysilane (OTES) (Gelest, Inc.) self-assembled monolayer (SAM) was deposited on the glass following the procedure described by Walba et al.[32] Briefly, clean glass slides were rinsed with acetone and toluene and submerged in a solution of toluene, OTES, and butylamine (200:3:1 v/v/v) for 30 min at 60 °C. Following, the glass slides were rinsed with toluene, dried with a stream of nitrogen, and stored under a vacuum at room temperature for 24 h prior to use. This produced a surface with a water contact angle of ∼95° as measured optically by the sessile drop method with a goniometer, sufficient to induce homeotropic alignment of the liquid crystal (LC). The slides were cut into small rectangles measuring approximately 0.25×0.20 in^2.

The LC material used was E7 ($n_\perp = 1.57$, $n_\parallel = 1.73$, Merck Ltd.), a four-component LC mixture of cyanobiphenyls and a cyanoterphenyl with a nematic to isotropic (N−I) transition temperature of 60 °C.[12] Octadecylammonium bromide (OTAB, Aldrich) dissolved in chloroform was added to the LC material, briefly mixed with a glass pipet, and then dried under a stream of nitrogen. The final concentration of OTAB in the LC was 100 ± 20 μM. The LC was drawn into a 25 μm capillary tube and used to fill a gilded TEM grid via capillary action by contacting the capillary tube to the grid laying flat on a rectangle of SAM-coated glass. The TEM grid (SPI Supplies) used was a gold-coated copper, square mesh grid with hole sizes of 205 μm. Following the introduction of the LC into the grid, the LC was heated above its nematic-to-isotropic transition temperature and slowly cooled back to room temperature. This resulted in an LC layer of approximately 20 μm in thickness.

Adsorption of ssDNA. Eight-well chamber slides (Laboratory-Tek) were filled with 500 μL of a solution consisting of 5 mM sodium chloride, 2.5 μM of 16-mer single-stranded DNA (ssDNA) oligonucleotides, AGAAAAAACTTCGTGC, (Operon), henceforth called sequence **A**, and up to 10% formamide, if used. The pH of this solution ranged from 5.5 to 6.0. LC-filled TEM grids on SAM-

(14) Price, A. D.; Schwartz, D. K. *J. Phys. Chem. B* **2007**, *111*, 1007–1015.
(15) Lockwood, N. A.; Abbott, N. L. *Curr. Opin. Colloid Interface Sci.* **2005**, *10*, 111–120.
(16) Brake, J. M.; Daschner, M. K.; Abbott, N. L. *Langmuir* **2005**, *21*, 2218–2228.
(17) Kaganer, V. M.; Mohwald, H.; Dutta, P. *Rev. Mod. Phys.* **1999**, *71*, 779–819.
(18) Brake, J. M.; Mezera, A. D.; Abbott, N. L. *Langmuir* **2003**, *19*, 6436–6442.
(19) Osica, V. D.; Pyatigorskaya, T. L.; Polyvtsev, O. F.; Dembo, A. T.; Kliya, M. O.; Vasilchenko, V. N.; Verkin, B. I.; Sukharevsky, B. Y. *Nucleic Acids Res.* **1977**, *4*, 1083–1096.
(20) Radler, J. O.; Koltover, I.; Salditt, T.; Safinya, C. R. *Science* **1997**, *275*, 810–814.
(21) Koltover, I.; Salditt, T.; Radler, J. O.; Safinya, C. R. *Science* **1998**, *281*, 78–81.
(22) Miller, A. D. *Angew. Chem., Int. Ed.* **1998**, *37*, 1768–1785.
(23) Sastry, M.; Ramakrishnan, V.; Pattarkine, M.; Gole, A.; Ganesh, K. N. *Langmuir* **2000**, *16*, 9142–9146.
(24) Erokhina, S.; Berzina, T.; Cristofolini, L.; Konovalov, O.; Erokhin, V.; Fontana, M. P. *Langmuir* **2007**, *23*, 4414–4420.
(25) Sukhorukov, G. B.; Montrel, M. M.; Retrov, A. I.; Shabarchina, L. I.; Sukhorukov, B. I. *Biosens. Bioelectron.* **1996**, *11*, 913–922.
(26) Kago, K.; Matsuoka, H.; Yoshitome, R.; Yamaoka, H.; Ijiro, K.; Shimomura, M. *Langmuir* **1999**, *15*, 5193–5196.
(27) Ramakrishnan, V.; Costa, M. D.; Ganesh, K.; Sastry, M. *J. Colloid Interface Sci.* **2004**, *276*, 77–84.
(28) Symietz, C.; Schneider, M.; Brezesinski, G.; Mohwald, H. *Macromolecules* **2004**, *37*, 3865–3873.
(29) Cardenas, M.; Nylander, T.; Jonsson, B.; Lindman, B. *J. Colloid Interface Sci.* **2005**, *286*, 166–175.
(30) Chen, X.; Wang, J.; Liu, M. *J. Colloid Interface Sci.* **2005**, *287*, 185–190.
(31) Brake, J. M.; Abbott, N. L. *Langmuir* **2002**, *18*, 6101–6109.

coated glass were submerged in the solution for 30−60 min, sufficient time for the LC/aqueous interface to reach a steady-state surface coverage. The solution was held constant at 25 °C throughout the formation of the interfacial layer. A cover was placed on the chamber to limit evaporation.

Polarized Light Microscopy. The LC orientation and textures were observed using plane-polarized light with an Olympus microscope (model BH2-UMA) modified for transmission mode incorporating crossed polarizers. The chamber slide containing the LC setup was placed on a rotating stage with an attached custom, liquid-based heating and cooling stage. The stage was located between the polarizers. All images were captured using a Lumenera (model Infinity 1-C) digital video camera mounted on the microscope and positioned so its x and y axes were aligned with those of the polarizer and analyzer. The 5× magnification was provided by an Olympus objective with plan-achromat design, a numerical aperature (NA), of 0.13 and working distance of 18.0 mm. Images were captured using Lumenera's Infinity Capture software. Homeotropic orientation was determined by the absence of transmitted light during a full 360° rotation of the sample. An image analysis program, ImageJ, was used to measure homeotropic coverage in the holes of the TEM grid. In the absence of homeotropic orientation, the zenithal tilt angle at the nematic/water interface was determined by comparing the observed colors to those on a Michel−Levy chart.[33] This yielded the birefringence, from which we were then able to determine $\theta_{n/w}$, the zenithal angle of the LC director at the nematic/water interface, from the following equation:

$$\Delta n_e = \frac{1}{\theta_{n/w} - \theta_{n/SAM}} \int_{\theta_{nSAM}}^{\theta_{n/a}} \frac{n_{||} n_{\perp} d\theta}{\sqrt{n_{||}^2 \cos^2\theta + n_{\perp}^2 \sin^2\theta}} - n_{\perp}$$

where Δn_e was the effective average birefringence, $n_{||}$ was the index of refraction for E7 parallel to the optical axis, and $n_{\perp}$ was the index of refraction for E7 perpendicular to the optical axis. $\theta_{n/SAM}$ was the zenithal angle of the LC director at the nematic/SAM interface and was assumed to always have a value of 0 (homeotropic anchoring). The azimuthal angle was determined by rotating the sample to extinction.

Fluorescence Microscopy. The custom-built fluorescence apparatus was based on a Nikon inverted microscope (model Eclipse TE2000) with a back-illuminated electron-multiplied EMCCD camera (model Cascade-II:512, Photometrics, Inc.) for photon detection. Epi-illumination was provided by a metal halide lamp (model EXFO X-Cite 120, EXFO Lifesciences & Industrial Division) with exposure time adjusted by a computer-controlled Uniblitz shutter (model VMM-D3, Oz Optics Ltd.). The 10× magnification was provided by a Nikon objective with a plan-Fluorite design, an NA of 0.30, and a working distance of 16.0 mm. Temperature was held constant using a Peltier-based heating and cooling stage (model TD60-STC20A, Instec Inc.) with a standalone temperature controller (model STC200, Instec Inc.). Metamorph 6.3 software (Molecular Imaging, Sunnyvale, CA) was used for the image acquisition/processing and shutter controls.

DNA Hybridization. For hybridization, a 16-mer target, GCACGAAGTTTTTTCT (sequence **A′**), was dissolved in 5 mM sodium chloride solution to a concentration of 100 nM and added in a given amount to the chamber. The melting temperature (T_m) of this target to the ssDNA probe **A** was calculated to be 32.12 °C in bulk solution in the presence of 50 mM monovalent cations.[34] The sample was held constant at 25 °C and observed with the polarizing or fluorescence microscope. Deionized water (resistivity = 18.2 MΩ·cm) was added to keep the water level constant, as needed. 6-FAM labeled on the 5′ end of the target (Operon) was used for the fluorescence experiments. For fluorescence microscopy experiments, the target DNA solution was exchanged for 5 mM NaCl solution following hybridization in order to reduce background fluorescence. Control experiments were performed with other 16-mers with various degrees of mismatch to probe **A**, including random, GGGCGGATGAGTCAGT (sequence **B**), two-base-pair mismatch (2bpmm), GCAGGAAGTTTATTCT (T_m = 13.15 °C),[34] and one-base-pair mismatch (1bpmm), GCACGAACTTTTTTCT (T_m = 17.58 °C).[34]

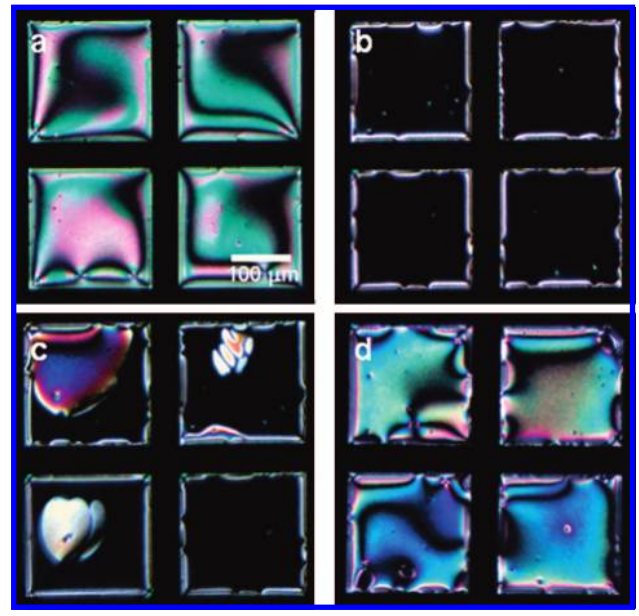

Figure 1. (a) LC appearance in the absence of OTAB when in contact with water. (b) Adsorption of OTAB at the LC/aqueous interface causes homeotropic alignment of the LC layer. (c) Birefringent regions appear upon exposure of the OTAB-laden interface to an ssDNA probe. (d) Birefringent regions expand until the holes are predominately birefringent.

Results

OTAB and ssDNA Adsorption. Following the immersion of the LC-filled grids into aqueous OTAB solution, the initially birefringent grid holes (Figure 1a) quickly became dark (homeotropic anchoring) as OTAB dissolved in the LC adsorbed and modified the structure of the nematic/aqueous interface (Figure 1b). For OTAB concentrations much smaller than described above, the grid holes remained birefringent, suggesting that a critical interfacial concentration of OTAB was required to trigger the change to homeotropic alignment.

If ssDNA probes (**A**) were also included in the aqueous solution, the rapid change to homeotropic anchoring was followed by a slower process where birefringent regions appeared and grew (Figure 1c). The birefringent domains displayed colors indicative of low effective birefringence (white, yellow, and orange in this case) with effective birefringence increasing as the domains continued to expand. Over the course of 30 min, the birefringent domains continued to form and merge until only small regions of homeotropic alignment remained (Figure 1d). At this point, the absolute effective birefringence of the cell was always relatively small, consistent with an intermediate anchoring angle in the range ∼35−55° depending on ssDNA concentration. Higher ssDNA concentrations resulted in larger birefringence/tilt angles; however, these changes were subtle and required dramatic changes in concentration. If no OTAB was dissolved in the LC, the ssDNA

(32) Walba, D. M.; Liberko, C. A.; Korblova, E.; Farrow, M.; Furtak, T. E.; Chow, B. C.; Schwartz, D. K.; Freeman, A. S.; Douglas, K.; Williams, S. D.; et al. *Liq. Cryst.* **2004**, *31*, 481–489.
(33) Robinson, P. C.; Davidson, M. W. Michel-Levy Interference Color Chart (http://www.microscopyu.com/articles/polarized/michel-levy.html), 2006.
(34) Oligo mismatch calculator (http://arep.med.harvard.edu/cgi-bin/adnan/tm.pl).

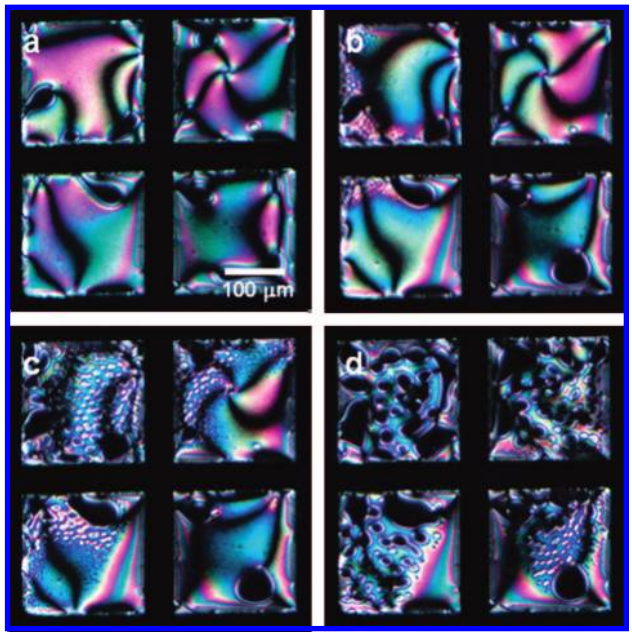

Figure 2. Hybridization of 1 pmol of ssDNA target to an OTAB/ssDNA interfacial layer. (a) No target. (b−d) Homeotropic domains appear and grow with time upon addition of complementary target. The steady-state appearance upon response saturation at long times is not shown.

probe in solution had no effect on the alignment of the LC, the textures being analogous to that of pure water, i.e., azimuthally disordered with high effective birefringence (Figure 1a).

Hybridization to Target Complement. The experimental arrangement described above permitted the direct observation of interfacial hybridization to a complementary target without additional preparation. In particular, it was not necessary to remove excess (unadsorbed) ssDNA probe from solution because the solution conditions were of sufficiently high stringency as to inhibit bulk hybridization.[35] Exposure of 1 pmol complementary target (**A′**) to the OTAB/ssDNA interface (Figure 2a) caused the sudden nucleation of small homeotropic domains (Figure 2b−d). The homeotropic domains appeared in a matter of seconds for picomole amounts of target; the response time was slowed to the order of minutes for femtomole amounts of target and for higher stringency conditions (i.e., addition of formamide as described below). The initially small homeotropic domains grew and coalesced, finally reaching a steady-state surface coverage of homeotropic alignment dependent on concentration of the target and conditions of the experiment.

The appearance of homeotropic regions was accompanied by a measurable increase in the birefringence of the remaining birefringent regions. For the case shown in Figure 3, the increase of birefringence corresponds to an increase of the zenithal tilt angle from $36 \pm 9°$ (Figure 3a) to $53 \pm 6°$ (Figure 3b) measured relative to the surface normal.

When fluorescently labeled target DNA was used, a comparison of images obtained using fluorescence and polarization microscopy revealed a direct correspondence between LC domains and the concentration of the target at the interface (Figure 4). In particular, the fluorescent ssDNA target was preferentially localized in the same lateral regions where the

(35) Kelsee, R. E. In *Basic DNA and RNA Protocols*, 2nd ed.; Harwood, A. J., Ed.; Humana Press: Totowa, NJ, 1996; pp 31−39..

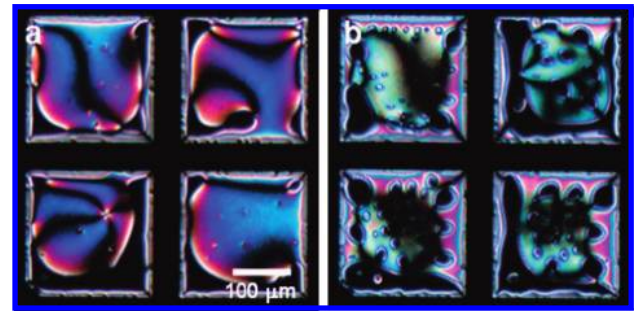

Figure 3. Nucleation of homeotropic domains caused the zenithal tilt angle in the birefringent regions to increase, as indicated by the rise in birefringence, i.e., zenithal tilt increases from (a) $36 \pm 9°$ to (b) $53 \pm 6°$.

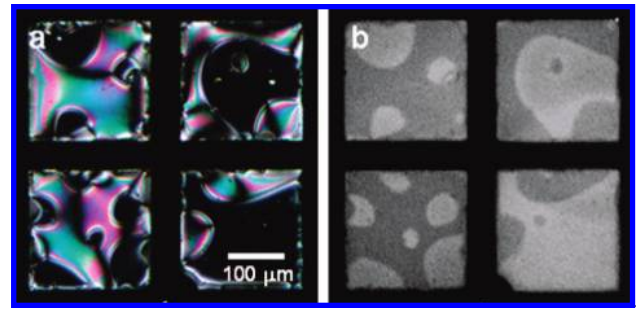

Figure 4. Domains following hybridization of 1 pmol of labeled-ssDNA complementary target to an OTAB/ssDNA interfacial layer. (a) Polarization microscopy. (b) Fluorescence microscopy; the bright regions indicate a higher concentration of labeled target.

LC layer was homeotropically aligned. This established a direct relation between target binding at the interface and LC alignment.

Sensitivity of DNA Recognition. We have chosen to express the sensitivity of the system to target DNA in terms of target dose in absolute molar amounts as opposed to solution concentration. We do believe that a dynamic equilibrium is achieved when the chemical potential of the bulk equals that of the interface. However, as we will show later, for the small volumes of the bulk aqueous phase used in these experiments, adsorption of ssDNA target to the interface significantly depleted the concentration of the solution, so it is impractical for us to express the sensitivity in terms of final equilibrium concentration.

Figure 5a−f show the LC response to incremental additions of 100 fmol of target. The limit of detection was ∼50 fmol, with a measurable increase in homeotropic coverage observed for 100 fmol of target. Between 50 and 400 fmol of target, there was a dramatic response to the target causing a significant increase in coverage by homeotropic regions for each 50−100 fmol addition. The response saturated at ∼500 fmol of target with additional target causing no increase in homeotropic coverage. As expected, the response time of the system was affected by sample volume. In particular, sample volumes > 500 μL resulted in noticeably slower kinetics limited by diffusive transport of target to the interface and decreased chemical potential of the bulk.

The LC response to ssDNA target was quantified by measuring the increase of the area fraction of homeotropic regions above the baseline prior to target addition. The dynamic response of the LC to target, Figure 6, was an S-curve typical for sensor response showing the limit of detection (∼50 fmol), dynamic range (100−500 fmol), and saturation of the response.

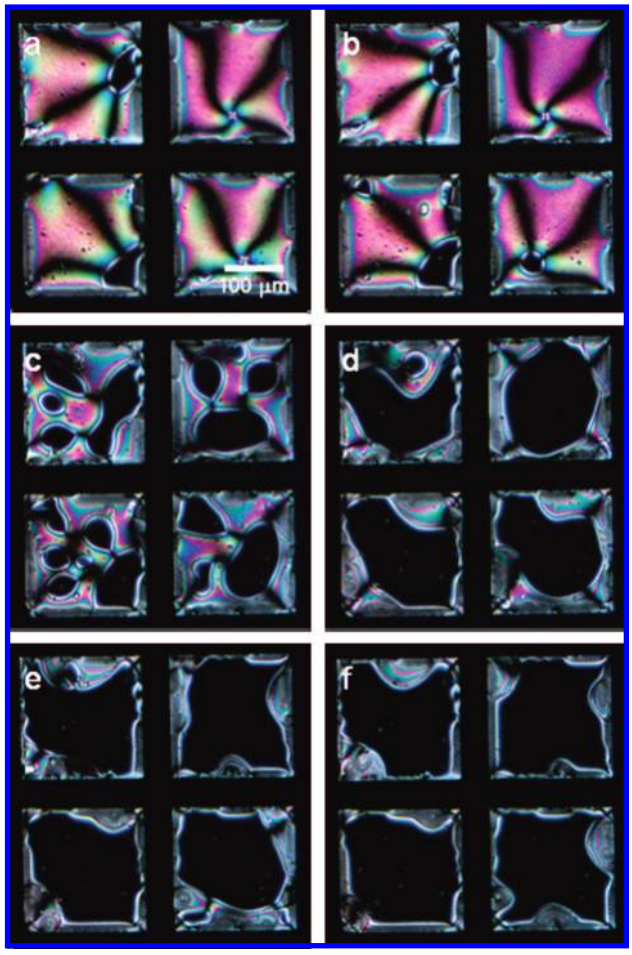

Figure 5. Surface coverage of homeotropic domains upon binding to (a) 0, (b) 100, (c) 200, (d) 300, (e) 400, and (f) 500 fmol of target.

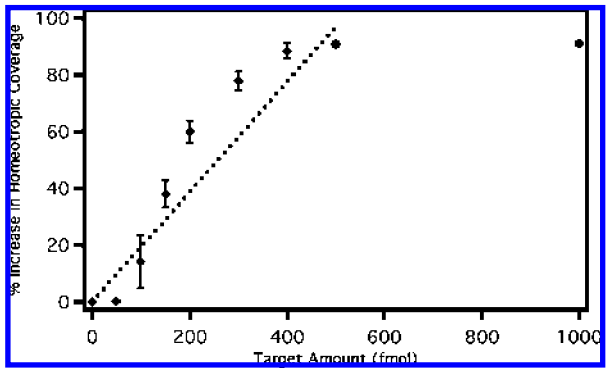

Figure 6. Dose−response curve for hybridization to the target. The dotted line represents the calculated close-packed area fraction of dsDNA assuming the interfacial hybridization of all target DNA as described in the text.

Specificity of DNA Recognition. The LC response to the DNA target was sensitive to base pair mismatches in the 16-mer targets. As an initial control, a random 16-mer (**B**) was investigated that was not expected to hybridize to the interfacial probe (**A**), even under highly favorable conditions. An excess of **B** was used to highlight the specificity of the response even for relatively large amounts of the mismatched target. Figure 7a shows the LC appearance following formation of an OTAB/ssDNA (**A**) interfacial layer. Addition of 25 pmol of **B** caused the birefringence to increase slightly (consistent with the increase in birefringence observed by increased amounts of probe), but

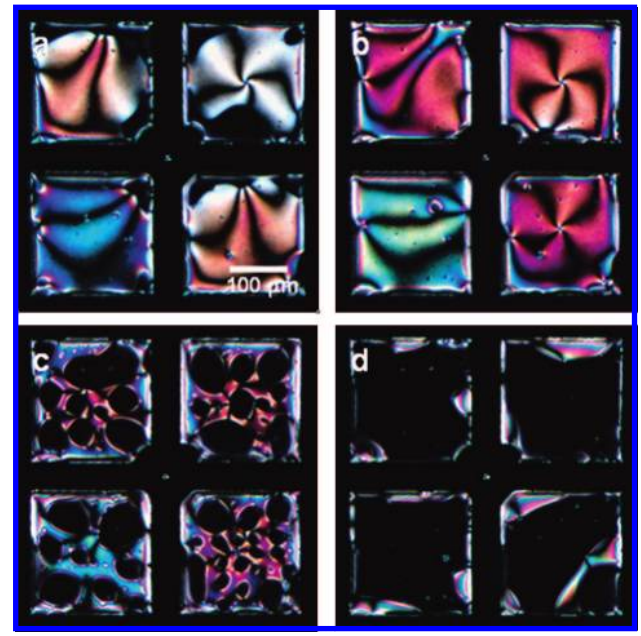

Figure 7. LC response to 16-mer target, **A′**, or 16-mer random sequence, **B**. (a) OTAB/**A** interfacial layer, (b) with 25 pmol of **B** added; (c) with 25 pmol of **B** + 25 pmol of **A′** added, 30 s after addition of **A′**; (d) with 25 pmol of **B** + 25 pmol of **A′** added, 25 min after addition of **A′**.

no homeotropic domains were observed to form (Figure 7b). Then 25 pmol of the complementary target, **A′**, were added to solution. Figure 7c and 7d show the LC response 30 s and 25 min following the addition of **A′**; the formation and coalescence of homeotropic domains were clearly observed. An identical experiment using **B** as the interfacial probe (not shown) responded similarly to its target, **B′**, demonstrating that response is independent of the oligonucleotide sequence.

Introducing one or more mismatches into the target inhibited hybridization, relative to a perfectly complementary target, by effectively lowering the melting temperature for hybridized DNA, assuming all other factors were kept constant. The melting temperature refers to the temperature at which the oligonucleotide is 50% annealed; generally it is calculated under standard solution conditions. Since the conditions in our experiments are very far from standard (in particular the ionic strength is very low), and the interfacial environment is unique, the calculated melting temperatures have no absolute meaning. However, the relative melting temperatures of the different targets provide a quantitative comparison of their annealing tendencies due to the number and location of base-pair mismatches in the target strand under a given set of experimental conditions. A two-base-pair mismatch (2bpmm, $T_m = 13.15$ °C) in 16 was enough to completely prevent an LC response for the conditions described above (25 °C, 5 mM NaCl). In this case, the LC response was similar to that of the random sequence, **B**. Specifically, the birefringence increased slightly when 50 pmol of 2bpmm was added but no homeotropic domains appeared. For 50 pmol of a one-base-pair mismatch (1bpmm, $T_m = 17.58$ °C) small homeotropic domains were observed to form near the edges of the grid holes (Figure 8a and b). Though significant, this response was dramatically decreased compared to a perfect match, which would have resulted in ∼90% homeotropic coverage. The inclusion of 8% formamide to the aqueous phase increased the stringency of the system by effectively lowering the melting temperature ∼6.0 °C and inhibited formation of homeotropic domains for 50 pmol of 1bpmm (Figure 8c and

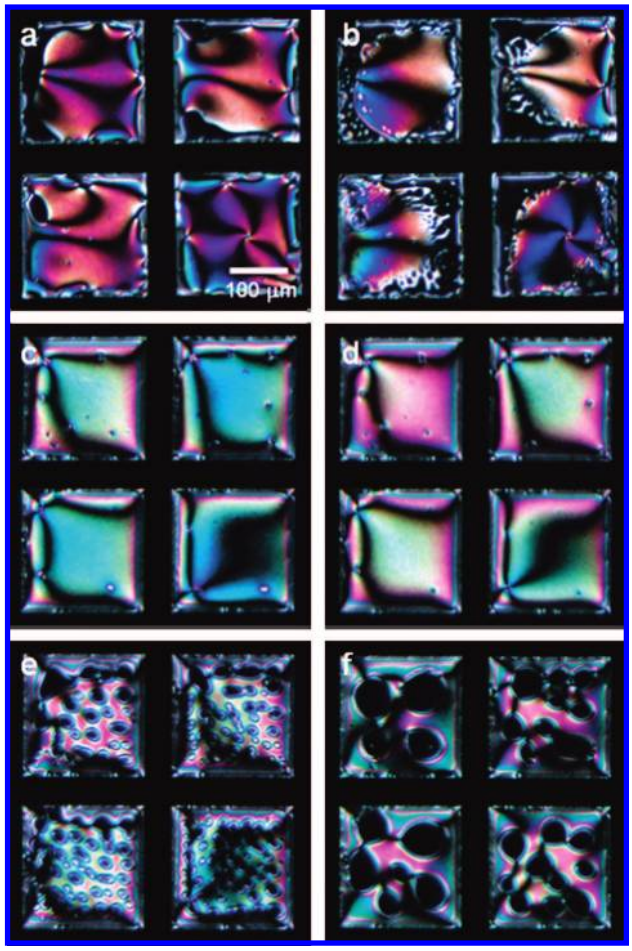

Figure 8. LC response to 16-mer target, **A′**, or 16-mer 1bpmm. (a) OTAB/**A** complex adsorbed at the LC/aqueous interface; (b) as in (a) with 50 pmol of 1bpmm added; (c) OTAB/**A** complex adsorbed at the LC/aqueous interface with 8% formamide; (d) as in (c) with 50 pmol of 1bpmm added; (e) as in (c) with 50 pmol of 1bpmm + 50 pmol of **A′** added, 1 min after addition of **A′**; (f) as in (c) with 50 pmol of 1bpmm + 50 pmol of **A′** added, 3 min after addition of **A′**.

d). Subsequent addition of 50 pmol of target, **A′**, caused the appearance, Figure 8e, and coalescence, Figure 8f, of homeotropic domains until 75−95% surface coverage by the homeotropic domains (not shown).

Discussion

Surfactant Adsorption. Past studies have shown that the adsorption and self-assembly of surfactant molecules at the interface between a liquid crystal and aqueous phase can modify the anchoring of the LC layer.[14,16] These studies suggested, in fact, that amphiphilic monolayers can form at this interface in analogy with those known to form at the air/water and oil/water interfaces[17] and that these monolayers can adopt various 2D phases as a function of thermodynamic conditions. Different phases have different LC anchoring properties. In particular, very dilute phases often result in tilted anchoring, while denser monolayers often result in homeotropic anchoring. Similarly, self-assembled monolayers deposited on solid surfaces also control LC anchoring,[36] with thicker, well-organized monolayers inducing homeotropic anchoring and thinner, more dilute monolayers inducing tilted/planar anchoring.[36] Molecular tilt within the surface layer may also influence LC anchoring; however, tilt is generally coupled to surface concentration in these systems.

While the experiments presented here do not represent rigorous proof of monolayer formation, given the amphiphilic nature of the OTAB molecules, it is certainly reasonable to expect that they will partition to the LC/water interface. The modification of LC anchoring reinforces this expectation. Furthermore, the absolute amount of surfactant added is small, precluding the possibility of homogeneous multilayer adsorption. In fact, if all of the OTAB dissolved were to adsorb at the interface, the average molecular area would be 0.85 nm^2/molecule, compared with a close-packed molecular area of ~0.25 nm^2. Therefore, the average surface concentration is less than one-third of a close-packed monolayer. We see no evidence of lateral heterogeneity, although we cannot rule out the possibility that this could occur at submicron length scales.

DNA Interaction with Surfactant-Laden Interface. In the current studies, the association between adsorbed OTAB and ssDNA in solution reorganized the structure of the surfactant-laden interface (Figure 1) causing a transition from homeotropic anchoring to tilted. Previous studies involving ssDNA interactions with Langmuir monolayers of cationic surfactant (octadecylamine, ODA; or cetyltrimethylammonium bromide, CTAB) indicated that an interfacial complex forms due to electrostatic interactions[23,24,37] and that surface-pressure vs area isotherms of the complex are shifted to larger molecular areas relative to the pure surfactant.[23] One interpretation of these findings is that the electrostatic binding of the ssDNA results in an effective increase in the size of the surfactant headgroup, due possibly to steric interactions or intercalation of the ssDNA into the headgroup layer. Also, although a shift to a larger average molecular area (i.e., a reduction of interfacial concentration) within the surfactant layer could explain our observations and seems to be consistent with Langmuir monolayer studies, this interpretation is problematic because the total area occupied by the interface is constant; one would have to hypothesize the loss of surfactant into an adjacent bulk phase. We speculate that the interaction of ssDNA with the adsorbed surfactant induces a subtle change in the structure of the surfactant layer (without a dramatic change in average interfacial concentration) inducing a change in LC anchoring. There is precedence for this type of phenomenon; we previously observed a temperature-driven structural change in a surfactant monolayer under constant-area conditions that induced a similar change in LC anchoring.[14] However, future work to characterize this structural change directly is clearly called for.

Interfacial DNA Hybridization. A significant result of these studies is that the cationic surfactant interface provides a local environment conducive to DNA hybridization. In bulk solution a high concentration of counterions (0.3−0.6 M) is necessary to screen electrostatic repulsion between DNA chains in order to promote hybridization;[35] however, the cationic interface apparently acts to neutralize the electrostatic repulsion between DNA even at low bulk ionic strength (5 mM NaCl). It is interesting to note that the nature of the cationic surfactant appeared to have a significant impact on the ability of target to hybridize at the interface. Specifically, while nucleation and growth of homeotropic domains were observed when using OTAB, similar domains did not appear when ODA was used

(36) Jérôme, B. *Rep. Prog. Phys.* **1991**, *54*, 391–451.

(37) Nicolini, C.; Erokhin, V.; Facci, P.; Guerzoni, S.; Ross, A.; Paschkevitsch, P. *Biosens. Bioelectron.* **1997**, *12*, 613–618.

as the cationic surfactant. Though surface pressure−area isotherm studies by Sastry indicated the formation of dsDNA at an ODA monolayer adsorbed at the air/water interface,[23] our results are consistent with those of Erokhina et al. that indicated denaturation of dsDNA into ssDNA at ODA monolayers but not at CTAB monolayers.[24] Possible reasons for this include the stability of ssDNA hydrogen bonded to the ODA monolayer and/or local modification of the water environment within a Debye length of the ODA due to protonation of the ODA headgroups.[38]

LC Response to DNA Hybridization. Once tilted anchoring was induced by addition of ssDNA, additional ssDNA did not qualitatively change the structure of the interface. However, the addition of even small amounts of complement caused a significant LC response. As observed in Figures 2 and 5, femtomole additions of the complementary ssDNA target caused nucleation, growth, and coalescence of LC homeotropic domains. Fluorescence experiments (Figure 4) confirmed that these homeotropic domains correspond to areas where the target accumulated at the interface. As discussed above, homeotropic anchoring is often associated with a concentrated surfactant layer. Thus, it is possible that hybridization of the DNA associated with the surfactant layer resulted in a local condensation of the interfacial layer. In fact, cationic surfactants are frequently used in the condensation and precipitation of DNA in solution.[19] The positively charged headgroups are electrostatically attracted to the phosphate backbone of the DNA molecule while hydrophobic interactions among the hydrocarbon tails condense the molecule.[39] Similar observations have been identified for cationic surfactant monolayers where dsDNA forms condensed domains at the air/water interface.[28,30] In the interfacial configuration, this condensation may be driven by either the increase in negative charge density due to hybridization or the conformational change of the probe ssDNA as it hybridizes with the target. In particular, the relatively hydrophobic bases that are exposed in ssDNA are tied up in dsDNA, and pi stacking of the bases in dsDNA has the added tendency of stabilizing and condensing the complex.

To put the sensitivity of the LC response into a molecular context, it is instructive to estimate the average surface density of dsDNA within the homeotropic regions. An upper limit can be calculated by assuming that all of the target in solution hybridizes to probe at the interface with no molecules overlapping or extending into the solution. For B-DNA, the most common helical form, the helix length is 0.34 nm/base pair with a diameter of 2.37 nm.[40] Assuming a flat-lying molecular orientation, these dimensions project an area of 12.9 nm^2/molecule. So for 50 fmol, the limit of detection, the maximum area occupied is 0.39 mm^2, while, for 500 fmol, the saturation of LC response, the maximum area is 3.9 mm^2. The open area in the TEM grid is approximately 4.0 mm^2, so the calculated upper limit of DNA surface coverage is 10% and 100% for 50 fmol and 500 fmol of target, respectively, as indicated by the dotted line in Figure 6. Notably, these values increase over the same range of target measured experimentally. While this should be regarded only as an order-of-magnitude estimate, it is consistent with the first-order approximation that the amount of homeotropic region created may be directly related to the area occupied by a relatively close-packed layer of dsDNA associated with the surfactant-laden interface.

Any molecular-level model of the response of this system must also explain the observation that the nucleation of homeotropic domains is accompanied by an increase in birefringence, and therefore LC tilt angle, in the coexisting birefringent region (Figure 3). One speculative interpretation would be that the increase of birefringence (and tilt) is consistent with a decrease of interfacial concentration in the birefringent regions. This would suggest that the homeotropic domains represent a higher-density surface phase (under the assumption of constant total interfacial concentration).

Conclusions

Polarization microscopy was used to observe LC anchoring coupled to structural changes of a cationic surfactant-laden interface upon interaction with ssDNA and subsequent hybridization to complementary ssDNA. The association of an ssDNA "probe" and the interface caused a structural change that reoriented the adjacent nematic LC from homeotropic to tilted alignment. The subsequent hybridization of complementary target ssDNA to the ssDNA/surfactant interfacial complex resulted in the nucleation of homeotropic domains, possibly due to the emergence of interfacial regions where the surfactant/DNA complex was condensed. Fluorescence microscopy confirmed that the ssDNA target was colocalized in the same regions as these homeotropic domains. The high stringency conditions of the bulk aqueous phase (low ionic strength) largely confined the hybridization reaction to the interface where the cationic surfactant neutralized the electrostatic repulsion between the probe and target. The sensitivity of the LC anchoring to the interfacial structure allowed for the detection of DNA 16-mers with a lower limit of ~50 fmol and the ability to differentiate a one-base-pair mismatch between the probe and target.

Acknowledgment. This work was supported by the Liquid Crystal Materials Research Center (NSF MRSEC, Award No. DMR-0213918). A.P. acknowledges support from a Department of Education GAANN fellowship.

JA0774055

(38) Batel, R.; Jaksic, Z.; Bihari, N.; Hamer, B.; Fafandel, M.; Chauvin, C.; Schroder, H. C.; Muller, W. E. G.; Zahn, R. K. *Anal. Biochem.* **1999**, *270*, 195–200.
(39) Ganesh, K. N.; Sastry, M. *J. Indian Inst. Sci.* **2002**, *82*, 105–112.
(40) Voet, D.; Voet, J. G.; Pratt, C. W. *Fundamentals of Biochemistry: Life at the Molecular Level*; Wiley: New York, 2006.